

To Cite: Bayram AB, Koç M, Akyürekli S, Kaleli M, 2021. Comparison of Structural and Electro-optical Properties of Thin Films Fabricated for Different Deposition Times Using TiO₂ Precursor Solutions with and without HCl by Ultrasonic Spray Pyrolysis. Journal of the Institute of Science and Technology, 11(2): 1102-1113.

Comparison of Structural and Electro-optical Properties of Thin Films Fabricated for Different Deposition Times Using TiO₂ Precursor Solutions with and without HCl by Ultrasonic Spray Pyrolysis

Ahmet Buğrahan BAYRAM¹, Murat KOÇ², Salih AKYÜREKLİ³, Murat KALELİ^{4*}

ABSTRACT: In this report, two different TiO₂ solutions with and without HCl were, firstly, prepared. Then, totally twelve number of thin film samples were obtained using these solutions for each of these two different group films by ultrasonic spray pyrolysis (USP). Of these twelve samples, each of the four was created at three different spray times (25, 50, 75 min), respectively, and they were annealed at 500 °C. Structural, morphological, and electro-optical properties of TiO₂ thin films were performed by X-ray diffractometer (XRD), scanning electron microscope (SEM), atomic force microscope (AFM), and ultraviolet-visible spectrophotometer (UV-VIS). It was seen that the HCl addition improves the crystallinity of the thin film samples dramatically even though at low deposition temperatures. HCl addition causes densification on the surface of the films and these films also exhibited the best morphological and structural properties compared to thin films without HCl. Also, the bandgap values of all thin films prepared with and without HCl decreases from 3.40 to 3.21 eV and 3.29 to 3.15 eV, respectively. Increase in the thickness of films by the addition of HCl plays a vital role on the morphological, structural, and electro-optical properties of the samples.

Keywords: Titanium dioxide (TiO₂), Ultrasonic spray pyrolysis, Solution engineering

¹ Ahmet Buğrahan BAYRAM ([Orcid ID: 0000-0002-7364-8559](https://orcid.org/0000-0002-7364-8559)) Süleyman Demirel University, Graduate School of Natural and Applied Sciences, Isparta, 32260, Turkey

² Murat KOÇ ([Orcid ID: 0000-0002-1048-6150](https://orcid.org/0000-0002-1048-6150)) Isparta University of Applied Sciences, Vocational School of Technical Sciences, Department of Electricity and Energy, Isparta, 3200, Turkey

³ Salih AKYÜREKLİ ([Orcid ID: 0000-0001-6005-667X](https://orcid.org/0000-0001-6005-667X)) Süleyman Demirel University, Innovative Technologies Application and Research Center, Isparta, 32260, Turkey

⁴ Murat KALELİ ([Orcid ID: 0000-0002-3290-2020](https://orcid.org/0000-0002-3290-2020)) Süleyman Demirel University, Department of Physics, Faculty of Art and Sciences, Isparta, 32260, Turkey

*Corresponding Author: Murat KALELİ, e-mail: muratkaleli@sdu.edu.tr

Bu çalışma Ahmet Buğrahan BAYRAM'ın Yüksek Lisans tezinden üretilmiştir.

INTRODUCTION

The metal oxide semiconductors, such as TiO₂, ZnO, and In/Sn-O₂ are very well-known and widely studied material for various applications. Among these TiO₂ is the material which is extensively studied much by the researchers compared to the other materials due to its high chemical stability over a wide pH range chemical structure, biocompatibility, physical, optical and electrical properties such as suitable energy band structure, crystal structure and morphology (Karunagaran et al., 2005). The thin film form of TiO₂ has many applications such as gas sensor (Bharathi, 2014), solar cells (Vaičiulis et al., 2012; Mao et al., 2016), photo catalysts (Haynes et al., 2017), environmental pollution control (Pelaez et al., 2012), and “self-cleaning” coatings (Guo et al., 2016).

TiO₂ thin films are fabricated by using different techniques such as magnetron sputtering (Mazur, 2017), e-beam evaporation (Jang et al., 2000), dip coating (Biswas et al., 2018), spin coating (Golobostanfard and Abdizadeh, 2013; Patil et al., 2018), spray pyrolysis (Deshmukh et al., 2006; Ranasinghe et al., 2018), and ultrasonic spray pyrolysis (USP) (Nakaruk et al., 2010; Taziwa and Meyer, 2017). Among these, ultrasonic spray pyrolysis is a more precise, controllable, repeatable, and economic technique by reducing material consumption up to 80%.

Some properties of TiO₂ thin films, such as electric, optical, crystal structure, and morphology, have been studied by many researchers in detail (Supekar et al., 2013; Tsega and Dejene, 2017). Out of these studies, the effect of hydrochloric acid (HCl) addition into precursor solution on the physical and chemical properties of TiO₂ thin films has not been studied much. A few of the researchers have studied similar subjects. Tsega and Dejene (2017) examined the effect of HCl on the formulation of TiO₂ nanocrystalline powders and improvement of its photoluminescence property. In this study, they prepared solution four different pH values. They found that crystal structure changed with HCl addition. They also showed that; while the HCl content increased the strain value increased and the crystallite size decreased (Tsega and Dejene, 2017). Lee and Liu worked out the acid-hydrolysis method to prepare TiO₂ sol-gel with TiCl₄ as a precursor and they showed that nano-sized TiO₂ crystal could be formed at low temperature by addition of HCl acid (Lee and Liu, 2002). Nakaruk et al. (2010) examined the effect of the ultrasonic spray pyrolysis deposition time of TiO₂ thin films by keeping constant the precursor solution concentration, flow rate and substrate temperature. They showed that the thickness of the films depends on the deposition time (Nakaruk et al., 2010). Ramírez - Santos et al. (2012) deposited TiO₂ thin films onto glass slides by the sol-gel method assisted with polyethylene glycol (PEG). They found that; PEG added precursor solution films were crack-free and formed a porous structure after annealing at 500 °C (Ramírez-Santos et al., 2012). Arunachalam et al. (2015) produced TiO₂ thin film by spray pyrolysis method for solar cell applications. In their study, Titanyl Acetylacetonate (Tiacaac) as a precursor solution of TiO₂ was prepared in three different molarity (0.05 M, 0.10 M and 0.15 M). They showed that the best crystallization was obtained at 0.10 M (Arunachalam et al., 2015).

In this study, two different TiO₂ solutions with and without HCl were prepared. Then, totally twelve number of thin film samples were obtained using these solutions for each of these two different group films by ultrasonic spray pyrolysis (USP). Of these twelve samples, each of the four was created at three different spray times (25, 50, 75 min), respectively, and they were annealed at 500 °C. The characterization of these two groups of thin film samples were conducted by XRD, SEM, AFM, and UV-VIS. Finally, the effect of deposition parameters, such as deposition time and HCl addition, and also annealing effect on the crystal structure, surface morphology, and electro-optical properties of these two TiO₂ thin films were investigated.

MATERIAL AND METHODS

Experimental set-up

Titanium dioxide thin films with and without HCl were fabricated for three different deposition times by using ultrasonic spray pyrolysis set-up (Figure 1). It consists of five main parts which are a nozzle (for spraying the solution), syringe (to load the solution), syringe pump (to adjust the flow rate of the solution), moving table (a plate, moving in XYZ-three dimensions, on which the nozzle is mounted), and two piezoelectric transducers one of which is replaced at the exit of the syringe and the other one at the entrance of the nozzle (separating the solution into microstructure droplets).

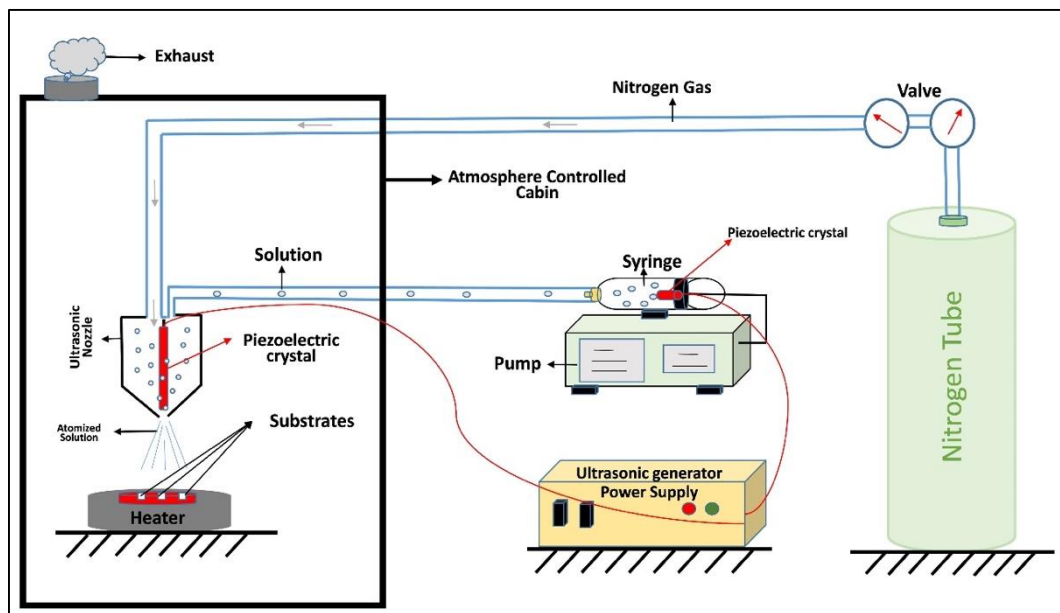


Figure 1. Schematic presentation of ultrasonic spray pyrolysis experimental set-up (Koç, 2018)

Preparation of thin film samples

We prepared two different TiO₂ thin film samples using two different solutions prepared with or without HCl using the starting materials 0.1 M Titanium (IV)-bis(acetylacetonat)-diisopropoxide (%75) (TiAcAc) (Merck, %75 solution in 2-propanol) solution as following: we first added 96.4 ml ethanol into 3.6 ml pure TiO₂ starting solution in a glass beaker and this mixture was mixed with a magnetic stirrer for 30 min. Then, we divided this solution into equally two parts and kept them in two separate beakers to use one of these solutions for the fabrication of pure TiO₂ thin film samples without HCl (or pure TiO₂ thin film) and the other one with HCl. Hence, we prepared the solution that we will use for the fabrication of the TiO₂ samples prepared with the solution including HCl. To obtain this solution, we added 0.2 ml HCl into the second and mixed this solution with a magnetic stirrer for 30 min. After preparing these two solutions, we prepared the 12 substrates for each of the thin film samples with and without HCl from microscope glass with suitable dimensions and cleaned them applying RCA standard cleaning method. After this step, we prepared the ultrasonic spray pyrolysis system to operate adjusting solution flow rate (0.5 ml/min), nozzle frequency (120 kHz), the distance between the substrate and the tip of the nozzle (10 cm), the substrate temperature (215 °C), and the nitrogen flow into the cabin. After completing these processes, we poured the first solution into the syringe and started the USP system to fabricate the thin film samples without HCl. To do it, we replaced 4 of 12 substrates on the table which will be used for four different characterization measurements and the solution sprayed 25 minutes. Following the same ways, we fabricated the other two groups of thin film samples applying the spraying

time 50 and 75 minutes, respectively. Similarly, thin film samples belonging to the second group of thin films were fabricated using the solution with HCl following the same way. The samples were coded as in Table 1.

Table 1. Codes of the fabricated TiO₂ thin film samples prepared without and with HCl for three different spraying times (25, 50, 75 min)

Sample Code	Number of the Samples	Samples fabricated without HCl			Samples fabricated with HCl		
		Spraying time (min)			Spraying time (min)		
		25	50	75	25	50	75
SA1	4	×	-	-	-	-	-
SA2	4	-	×	-	-	-	-
SA3	4	-	-	×	-	-	-
SB1	4	-	-	-	×	-	-
SB2	4	-	-	-	-	×	-
SB3	4	-	-	-	-	-	×

On the other hand, since the thin film samples with and without HCl were thermally annealed at 500 °C and the new form of codes of the samples were presented as SA1-T, SA2-T, SA3-T, SB1-T, SB2-T and SB3-T adding, respectively. After completing all these thin film deposition processes, it was realized the characterization of these samples.

Characterization of thin film samples

For the determination of the crystal structure of the samples, XRD measurements were conducted by using Cu-K α radiation source at a setting of 40 mA and 40 kV (Bruker D8 Advanced Twin-twin system). XRD Spectra of the films were recorded by scanning 2θ in the range 20-80°. Surface topography, elemental composition and thickness of the TiO₂ thin films samples were studied by scanning electron microscope (SEM) system (SEM: FEI Quanta FEG 250 – EDS: EDAX). The surface topology and roughness of the films were characterized by atomic force microscope (AFM) system (Nanomagnetics ez-AFM) with Si cantilever and tapping mode. The electro-optical properties of the TiO₂ films were characterized with a UV-VIS spectrophotometer (UV-VIS) (Perkin Elmer Lambda 950 UV/Vis).

RESULTS AND DISCUSSION

XRD measurements

Figure 2 a, b, and c, d show the XRD patterns of the samples (SA1, SA2 and SA3) as-grown and (SA1-T, SA2-T and SA3-T) thermally annealed at 500 °C and samples (SB1, SB2 and SB3) as-grown and (SB1-T, SB2-T and SB3-T) thermally annealed at 500 °C, respectively. As seen from Figure 2a, it is not seen any crystallization in each of the samples (SA1, SA2, and SA3), but in Figure 2b it is seen that crystallization in the samples (SA1-T, SA2-T and SA3-T) begins to appear and increases with the increasing of spraying time. These two results are the expected results. On the other hand, as seen from Figure 2c, it is not seen any crystallization in each of the samples (SB1, SB2, and SB3), but in Figure 2d it is seen that crystallization in the samples (SB1-T, SB2-T and SB3-T) begins and increases with the increasing of spraying time as expected. When the results obtained for the samples (SA1, SA2 and SA3) and (SB1, SB2 and SB3) not annealed are compared, it will be seen that there is no difference between them. Crystallizations are not good in both of these as-grown samples.

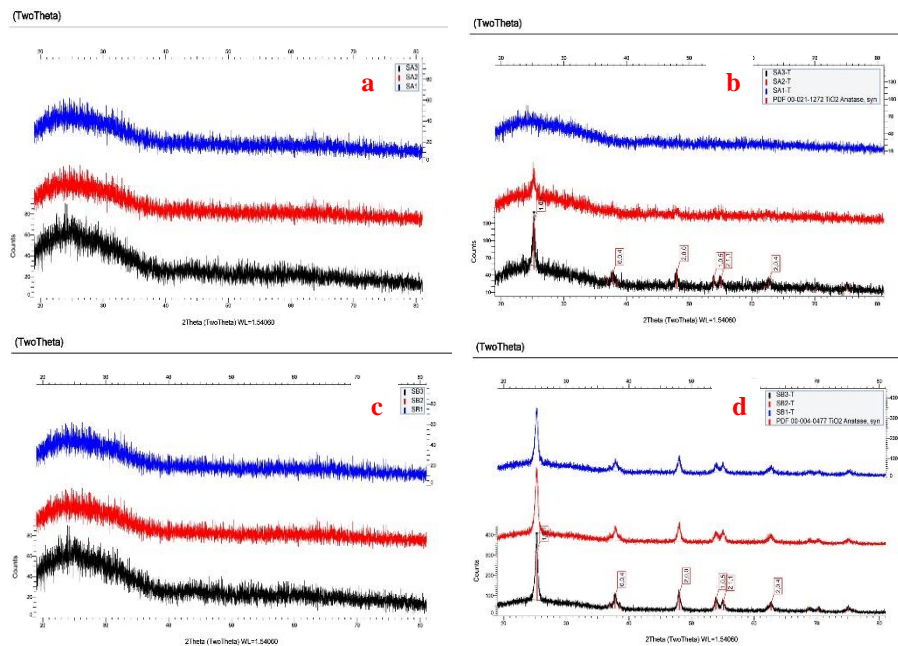


Figure 2. a, b, and c, d are the XRD patterns of the samples (SA1, SA2 and SA3) as-grown and (SA1-T, SA2-T and SA3-T) thermally annealed at 500 °C and samples (SB1, SB2 and SB3) as-grown and (SB1-T, SB2-T and SB3-T) thermally annealed at 500 °C, respectively

On the other hand, it is seen that the best crystallization forms in (SB1-T, SB2-T and SB3-T) samples. As seen from Figure 2d, the peaks appear at 2θ angles 25.3, 37.8, 48, 53.9, 54.8, 62.5 degrees and they are directed in the direction of planes (101), (004), (200), (105), (211), and (204), respectively. The type of the crystal structure of the samples was determined by means of PDF 00-021-1272 and PDF 00-004-0477 libraries and the obtained results showed that the samples have anatase phase. And also, all samples have a polycrystalline structure. This result is confirmed by some studies in the literature (Lee and Liu, 2002; Ramírez-Santos et al., 2012; Arunachalam et al., 2015; Tsega and Dejene, 2017; Biswas et al., 2018).

SEM measurements

Figure 3. a, b, c, d, e and f show the SEM images of (SA1-T, SA2-T, and SA3-T) and (SB1-T, SB2-T, and SB3-T) samples annealed at 500 °C. The films without HCl are seen that their highly porous surface is covered with a lot of micro-sized TiO₂ spheres of whereas the films formed in the presence of HCl are cracked but dense structure just a few numbers of micro-sized TiO₂ spheres on the dense surface. When the particle size decreases to the nanometer size, surface activities and surface areas increase due to the increase in the number of surface atoms.

Nanoparticles tend to be uncontrolled agglomeration forming with spherical shapes due to their high surface energies (Li et al., 1999). On the other hand, HCl addition also decreases the droplet shadows on the film surfaces. It is clear from the SEM images that HCl addition to precursor solution increases the densification of the films and this is confirmed with our XRD results. It is evident that HCl addition modifies both the surface morphology and the structure of the films.

Figure 4. a, b, and c and d, e, and f show the cross-section SEM images of the SA1-T, SA2-T, and SA3-T samples and SB1-T, SB2-T, and SB3-T samples, respectively. The measured film thickness values of the samples are given in Table 2.

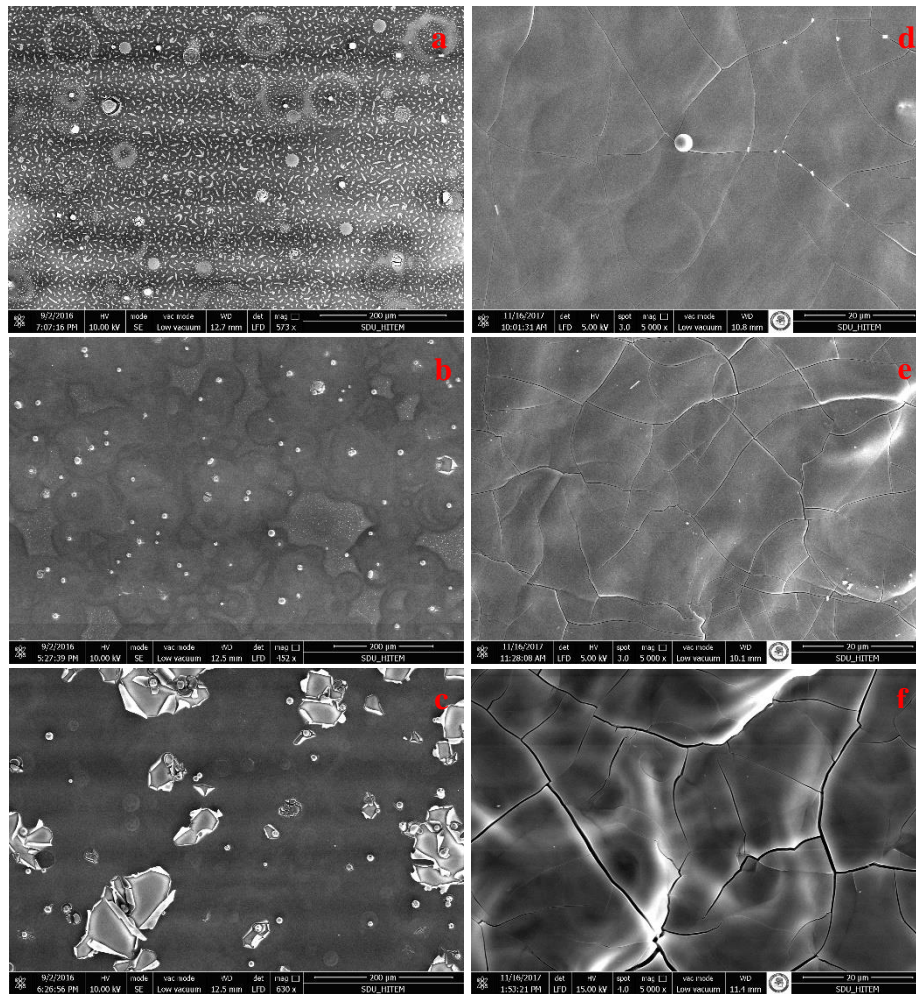


Figure 3. SEM images of (a) SA1-T, (b) SA2-T, and (c) SA3-T samples and (d) SB1-T, (e) SB2-T, and (f) SB3-T samples

Table 2. The film thickness of the SA1-T, SA2-T, and SA3-T and SB1-T, SB2-T, and SB3-T samples

Sample code	TiO ₂ without HCl Annealed at 500 °C			TiO ₂ with HCl Annealed at 500 °C		
	SA1-T	SA2-T	SA3-T	SB1-T	SB2-T	SB3-T
Thickness of the film (µm)	0.48	0.75	1.40	1.90	2.50	3.80

When the samples being in the same group are compared with each other, it is obvious that their thicknesses increase with spraying time. This result is normal and it may be said that it is an expected result. On the other hand, when the samples, taking place in two separate groups, fabricated at the same spraying time and thermally annealed at the same temperature are compared with each other, it is evident that the thicknesses of the samples with HCl are much larger than the samples without HCl. In this case, it may be said that use of the HCl in the solution plays a vital role on the thickness of the TiO₂ thin films. Solvent engineering plays a vital role for solution-based production techniques. HCl addition to the solution changes the physicochemical properties of the precursor solution by means of density, evaporation temperature, PH values and etc. SEM surface and cross-section images show that the solution drops evaporate before arriving the surface of substrate and then being blown away by the spray gas and this lead to formation of TiO₂ nanoparticles which doesn't interact with substrate surface (Vaiculis et al., 2012). These are clue for micro-sized TiO₂ sphere formation on the surface for pure TiO₂ precursor solution and thick film formation for HCl added precursor solution.

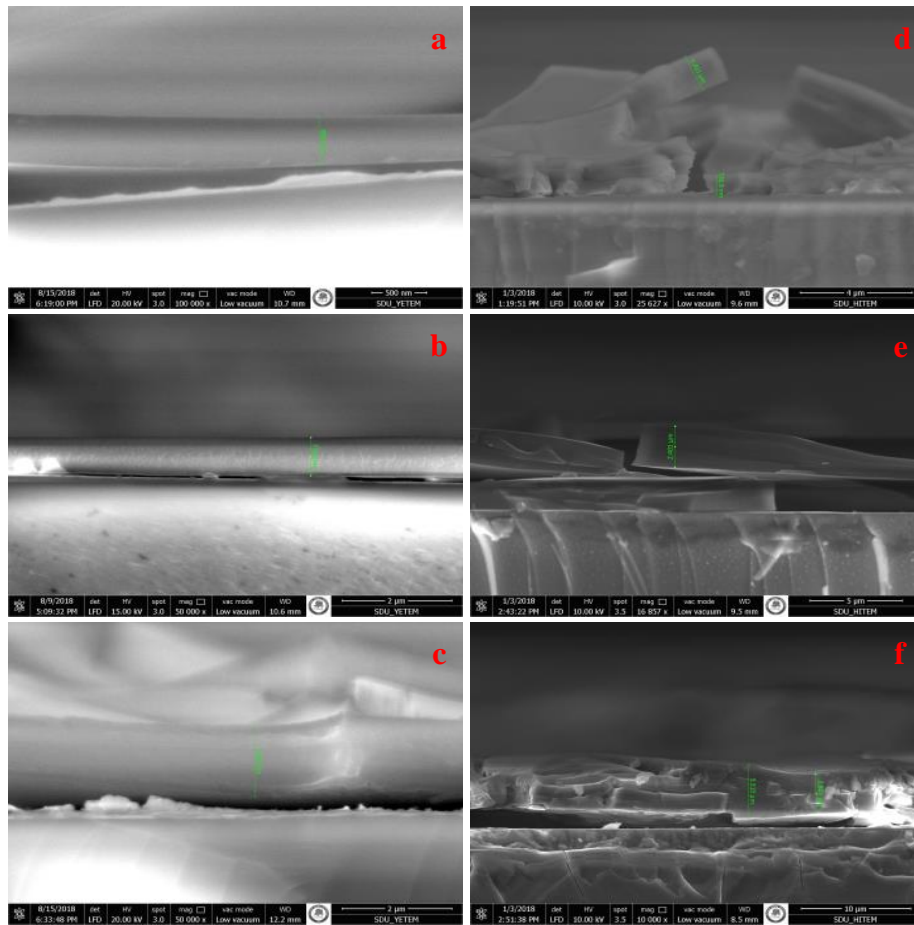


Figure 4. Cross-sectional SEM images of (a) SA1-T, (b) SA2-T, and (c) SA3-T samples and (d) SB1-T, (e) SB2-T, and (f) SB3-T samples

AFM measurements

AFM images of (a) SA1-T, (b) SA2-T, and (c) SA3-T samples and (d) SB1-T, (e) SB2-T, and (f) SB3-T samples are given in Figure. 5 a, b, c and d, e, f, respectively. When the samples SA1-T, SA2-T, and SA3-T are compared with each other, it is seen that their surface morphologies are nearly similar with each other.

Almost all of them have a lumpy surface structure. But, when the samples SB1-T, SB2-T, and SB3-T are compared with each other, it is seen that their surface morphologies differ from each other. While SB1-T has a surface morphology with cracks, cracks turn into valleys in sample SB2-T and surface morphology of the sample SB3-T turns into a surface formed with longitudinally cut cylinders. It will be seen that there is much difference between these two group samples when they are compared with each other.

Roughness (R_a) values of the annealed samples (SA1-T, SA2-T and SA3-T) without HCl are 1.51, 1.65, and 3.14 nm and the samples (SB1-T, SB2-T and SB3-T) with HCl are 83.0, 104, and 128 nm, respectively. HCl addition to precursor solution increased the R_a values dramatically by creating the sharp cracks (channels into blocks). This R_a increment may improve the TiO₂ thin films solar cell efficiency by increasing the active surface area.

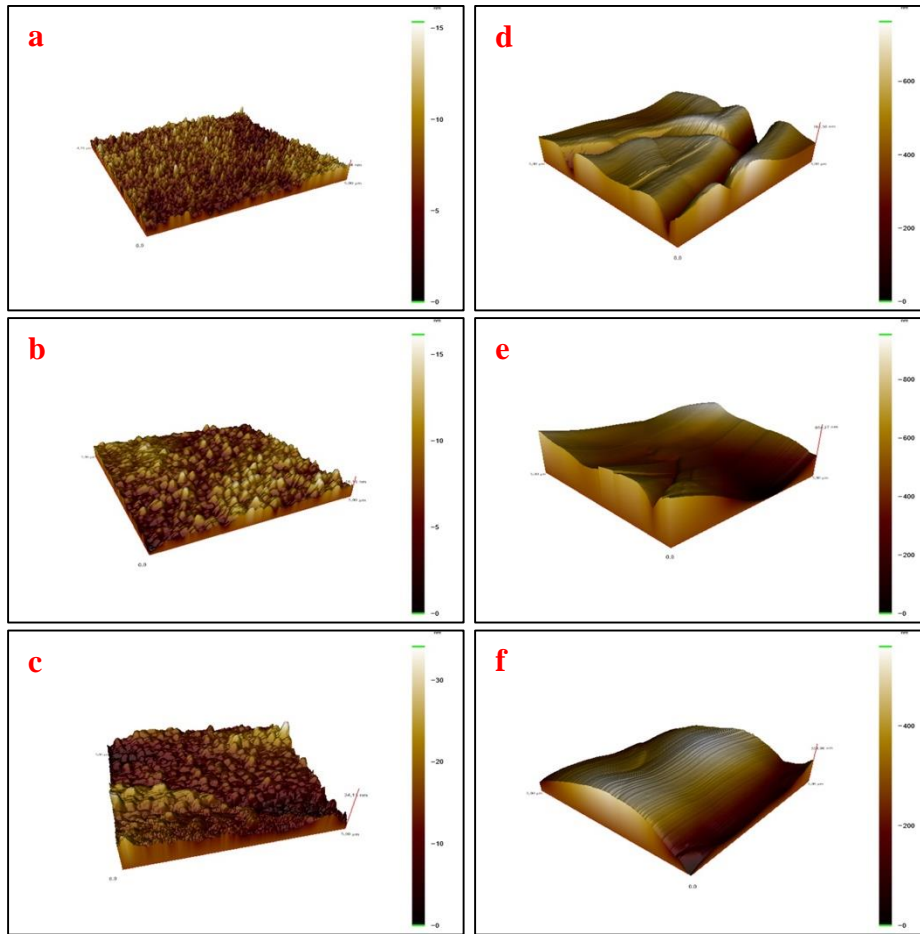


Figure 5. AFM images of (a) SA1-T, (b) SA2-T, and (c) SA3-T samples and (d) SB1-T, (e) SB2-T, and (f) SB3-T samples are given in Figure. 4 a, b, c and d, e, f, respectively

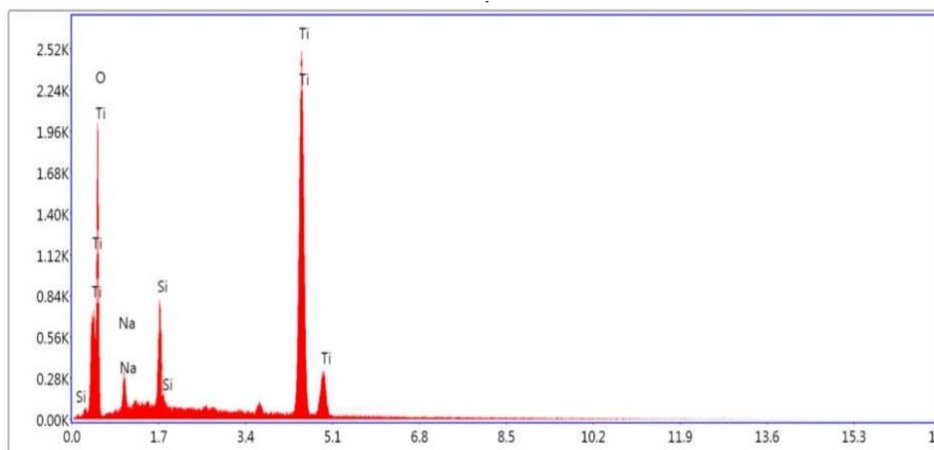


Figure 6. EDS spectrum of SB3 sample which presenting the composition of the elements included in the film

Table 3. Elements existing in the samples (SA1-T, SA2-T and SA3-T) and (SB1-T, SB2-T and SB3-T) and their percentages

Sample code	TiO ₂ without HCl Annealed at 500 °C			TiO ₂ with HCl Annealed at 500 °C		
	SA1-T	SA2-T	SA3-T	SB1-T	SB2-T	SB3-T
Elements (%)						
O	54.3	53.2	53.8	67.1	64.9	66.4
Ti	1.5	4.1	7.0	20.9	24.3	26.5

Figure 6 shows the EDS picture of SB3 sample and the graphics presenting the composition of the elements included in the sample. The same measurements were performed the other samples and the measured percentage values of O and Ti elements in all samples are given in Table 3. The existence of the Ti and O elements are expected resulting from TiO₂ thin films. But Si and Na are ingredients of the glass substrates.

UV-VIS measurements

Band gap energy values of the samples were found using the data from the UV-VIS measurements. To do this, transmittance curves of the samples versus wavelength of the photon and we calculated the absorption coefficient, α_i , corresponding to $h\nu_i$ (photon energy) using the following equation,

$$\alpha_i = \frac{1}{d} \ln \frac{1}{T} \quad (1)$$

where d and T are the thickness and the transmittance of the film, respectively. On the other hand, the energy band gap is found substituting the value of α into the equation (Ramírez-Santos et al., 2012; Golobostanfard and Abdizadeh, 2013; Chandrasekhar et al., 2016),

$$(\alpha h\nu)^n = A(h\nu - E_g) \quad (2)$$

where E_g is the bandgap energy value of the sample. For the bandgap calculations, the n value was chosen as $1/2$ since TiO₂ has an indirect bandgap. According to this equation, to find the bandgap energy values of the TiO₂ thin film samples a graph of $(\alpha h\nu)^{1/2}$ versus $h\nu$ has been plotted and then an extrapolation was applied to this graph. So, we drew a line lying on the part of the curve with a constant slope and cutting the $h\nu$ versus. The point cut by this line gives the band gap energy of the sample.

Figure 7. a and b show the $(\alpha h\nu)^{1/2}$ versus $h\nu$ plots of SA1-T, SA2-T, SA3-T, and SB1-T, SB2-T, SB3-T, respectively. As seen from Figure 7. a and b, the bandgap of the TiO₂ thin films with and without HCl are ranging in between decreasing from 3.29 to 3.15 eV and 3.40 to 3.21 eV, respectively which are consistent with literature (Nakaruk et al., 2010; Golobostanfard and Abdizadeh, 2013; Essalhi et al., 2016).

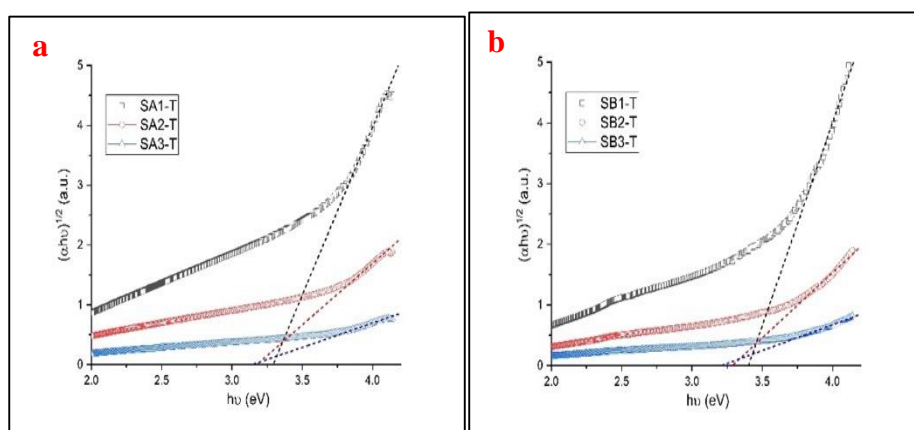


Figure 7. Graphics of $(\alpha h\nu)^{1/2}$ versus $h\nu$ show the band gap energies of the samples (a) SA1-T, SA2-T and SA3-T and (b) SB1-T, SB2-T and SB3-T

This result can be explained as following: by increasing deposition time of the films with or without HCl addition to precursor solution, a redshift on the absorption edge of the TiO₂ films occurred, which involved a decrease of the bandgap energies. Increasing the film thickness results a band gap

decrease and absorption increase and this effects can be seen for a lots of previous TiO₂ thin film studies (Nakaruk et al., 2010; Golobostanfard and Abdizadeh, 2013).

Table 4. Band gap values for the samples (SA1-T, SA2-T and SA3-T) without HCl and the samples (SB1-T, SB2-T and SB3-T) with HCl annealed at 500 °C

Sample code	TiO ₂ without HCl Annealed at 500 °C			TiO ₂ with HCl Annealed at 500 °C		
	SA1-T	SA2-T	SA3-T	SB1-T	SB2-T	SB3-T
Band gap (eV)	3.29	3.17	3.15	3.40	3.28	3.21

CONCLUSIONS

In this project, TiO₂ thin films with and without HCl were deposited by ultrasonic spray pyrolysis system for three different spraying times (25, 50, 75 min) and the surface morphology, structural, electro-optical, and chemical composition of the films were investigated by means of SEM, AFM, XRD, UV-VIS, and EDS. SEM images of the films without HCl showed that the thicknesses of the films increased with spraying time and with the addition of the HCl increased the film thickness too. But the thickness of the thin films with HCl are larger compared to the samples without HCl. On the other hand, AFM images showed that the roughness of the samples with HCl are larger compared (~1.51 nm and 128 nm) the films without HCl. UV-VIS measurements indicated that the bandgap energy value of the films without HCl have a maximum and minimum band gap energy values are 3.29 and 3.15 eV while thin with HCl have a maximum and minimum band gap energy values are 3.40 and 3.21 eV. As a result, it can be said that the bandgap energy values of both of these thin film samples decreases to ~3.2 eV with the increase of the thickness.

The XRD analysis shows that TiO₂ films crystallize in anatase phase with the (101) preferred orientation at 500 °C annealing temperature and the HCl addition improve the crystallization of the films sharply. HCl addition favors faster crystalline phase formation compared to pure TiO₂ precursor solution. In EDS measurements it is seen that the pyrolysis completely removed the HCl from the structure causing a quality improvement of the crystallinity of the samples. As a result, it can be said that the addition of HCl to precursor solution plays a vital role on the thin films morphology, structure and electro-optical properties. Additionally, we are going to study the effect of the HCl addition with different concentration with changing the height of the nozzle from the plate, atomizing frequency, and substrate temperature on the morphology, structural, electro-optical properties of the TiO₂ thin films.

ACKNOWLEDGMENT

This project was supported by Süleyman Demirel University “Scientific Research Projects Coordination Unit (S.D.U S.R.P. 4899-YL1-17)”. We also thank Prof. Dr. Refik KAYALI for his help in proofreading the manuscript.

Conflict of Interest

The article authors declare that there is no conflict of interest between them.

Author's Contributions

The authors declare that they have contributed equally to the article.

REFERENCES

- Arunachalam A, Dhanapandian S, Manoharan C, Sridhar R, 2015. Characterization of Sprayed TiO₂ on ITO Substrates for Solar Cell Applications. *Spectrochimica Acta Part A: Molecular and Biomolecular Spectroscopy*. Elsevier B.V., 149, pp. 904–912.

- Bharathi JJ, Pappayee N, 2014. Titanium Dioxide (TiO₂) Thin Film Based Gas Sensors. National Conference on Green Engineering and Technologies for Sustainable Future, pp. 59-61.
- Biswas S, Rahman KH and Kar AK, 2018. Optical Properties of Titanium di-oxide Thin Films Prepared by Dip Coating Method. 2nd International Conference on Condensed Matter and Applied Physics AIP Conf. Proc. 1953, pp. 030004-1–030004-4.
- Chandrasekhar PS, Kumar N, Swami SK, Dutta V, Komarala VK, 2016. Fabrication of Perovskite Films Using an Electrostatic Assisted Spray Technique: The Effect of the Electric Field on Morphology, Crystallinity and Solar Cell Performance. *Nanoscale*. Royal Society of Chemistry, 8(12), pp. 6792–6800.
- Deshmukh HP, Shinde PS, Patil PS, 2006. Structural, Optical and Electrical Characterization of Spray-Deposited TiO₂ Thin Films. *Materials Science and Engineering: B*, 130(1–3), pp. 220–227.
- Essalhi Z, Hartiti B, Lfakir A, Siadat M, Thevenin P, 2016. Optical Properties of TiO₂ Thin Films Prepared by Sol Gel Method. *J. Mater. Environ. Sci.*, 7 (4), pp. 1328-1333.
- Golobostanfard MR, Abdizadeh H, 2013. Effects of Acid Catalyst Type on Structural, Morphological, and Optoelectrical Properties of Spin-Coated TiO₂ Thin Film. *Physica B: Condensed Matter*. Elsevier, 413, pp. 40–46.
- Guo MZ, Maury-Ramirez A, Poon CS, 2016. Self-Cleaning Ability of Titanium Dioxide Clear Paint Coated Architectural Mortar and Its Potential in Field Application. *Journal of Cleaner Production*. Elsevier Ltd, 112, pp. 3583–3588.
- Haynes VN, Ward JE, Russell BJ, Agrios AG, 2017. Photocatalytic Effects of Titanium Dioxide Nanoparticles on Aquatic Organisms-Current Knowledge and Suggestions for Future Research. *Aquatic Toxicology*. Elsevier B.V., 185, pp. 138–148.
- Jang HK, Whangbo SW, Choi YK, Chung YD, Jeong K, Whang CN, 2000. Titanium Oxide Films on Si(100) Deposited by E-beam Evaporation. *Journal of Vacuum Science & Technology A: Vacuum, Surfaces, and Films*, 18(6), pp. 2932–2936.
- Karunakaran B, Chung SJ, Suh EK, Mangalaraj D, 2005. Dielectric and Transport Properties of Magnetron Sputtered Titanium Dioxide Thin Films. *Physica B: Condensed Matter*, 369(1–4), pp. 129–134.
- Koç M, 2018. Investigation of Physical and Optical Properties Sn-Doped Indium Oxide Thin Films Fabricated by Ultrasonic Spray Pyrolysis Method and Heat Treatment under Different Nitrogen Flow Rate Atmospheres. Süleyman Demirel University, Graduate School of Natural and Applied Sciences, PhD Thesis (Printed).
- Lee DS, Liu TK, 2002. Preparation of TiO₂ Sol Using TiCl₄ as A Precursor. *Journal of Sol-Gel Science and Technology*, 25(2), pp. 121–136.
- Li B, Xie Y, Huang J, Su H, Qian Y, 1999. Solvothermal Synthesis to NiE₂ (E = Se, Te) Nanorods at Low Temperature. *Nanostructured Materials*, 11(8), pp. 1067–1071.
- Mao X, Zhou R, Zhang S, Ding L, Wan L, Qin S, Chen Z, Xu J, Miao S, 2016. High Efficiency Dye-sensitized Solar Cells Constructed with Composites of TiO₂ and the Hot-bubbling Synthesized Ultra-Small SnO₂ Nanocrystals. *Scientific Reports*. Nature Publishing Group, 6(1), p. 19390.
- Mazur M, 2017. Analysis of the Properties of Functional Titanium Dioxide Thin Films Deposited by Pulsed DC Magnetron Sputtering with Various O₂:Ar Ratios. *Optical Materials*. Elsevier Ltd, 69, pp. 96–104.
- Nakaruk A, Ragazzon D, Sorrell CC, 2010. Anatase Thin Films by Ultrasonic Spray Pyrolysis. *Journal of Analytical and Applied Pyrolysis*. Elsevier B.V., 88(1), pp. 98–101.
- Patil NB, Nimbalkar AR, Patil MG, 2018. ZnO Thin Film Prepared by a Sol-gel Spin Coating Technique for NO₂ Detection. *Materials Science and Engineering: B*. Elsevier, 227(2), pp. 53–60.
- Pelaez M, Nolan NT, Pillai SC, Seery MK, Falaras P, Kontos AG, Dunlop PSM, Hamilton JWJ, Byrne JA, O'Shea K, Entezari MH, Dionysios DD, 2012. A review on The Visible Light Active Titanium Dioxide Photocatalysts for Environmental Applications. *Applied Catalysis B: Environmental*. Elsevier B.V., pp. 331–349.
- Pradhan UU, Kumar, SKN, 2011. Characterization of Titanium Dioxide Thin Film Fabricated Using Spin Coating Technique. *Optoelectronics and Advanced Materials*. 5(7), pp. 799–801.
- Ramírez-Santos AA, Acevedo-Peña P, Córdoba EM, 2012. Enhanced Photocatalytic Activity of TiO₂ Films by Modification with Polyethylene Glycol. *Química Nova*, 35(10), pp. 1931–1935.
- Ranasinghe CSK, Vequizo JJM, Yamakata A, 2018. Fabrication of Robust TiO₂ Thin Films by Atomized Spray Pyrolysis Deposition for Photoelectrochemical Water Oxidation. *Journal of Photochemistry and Photobiology A: Chemistry*. Elsevier BV, 358, pp. 320–326.
- Supekar AK, Bhise RB, Thorat SS, 2013. Optical, Structural and Morphological Study of TiO₂ Thin Film Using Sol-gel Spin Coating Techniques. *IOSR Journal of Engineering*, 3(1), pp. 38-41.

- Taziwa R, Meyer E, 2017. Fabrication of TiO₂ Nanoparticles and Thin Films by Ultrasonic Spray Pyrolysis: Design and Optimization. Pyrolysis, Intech, Open Science, pp. 223-249.
- Tsega M, Dejene FB 2017. Influence of Acidic pH on The Formulation of TiO₂ Nanocrystalline Powders with Enhanced Photoluminescence Property. Heliyon Elsevier Ltd., 3(2), pp. e00246.
- Vaiciulis I, Girtan M, Stanculescu A, Leontie L, Habelhames F, Antohe S, 2012. On Titanium Oxide Spray Deposited Thin Films for Solar Cells Applications. Proceedings of the Romanian Academy Series a-Mathematics Physics Technical Sciences Information Science, 13(4), pp. 335–342.